博士論文（要約）

Ocean wind and flight behavior of soaring seabirds investigated using high resolution flight records

（海鳥の高解像度飛行データに基づく海上風推定および飛翔行動特性の解明）

米原　善成

Yoshinari Yonehara

Index

Chapter 1

General Introduction

本章（項）の内容は、学術雑誌論文として出版する計画があるため公表できない。5年以内に出版予定。

Chapter 2

Wind estimation and verification using flight paths of seabirds soaring over the ocean surface

Introduction

Fine-scale wind information in the context of movement ecology of seabirds

Majority of flying animals are exposed to winds that have a significant effect in shaping their movements (Liechti, 2006). Soaring seabirds are most exposed to winds because they repeat thousands of kilometers of commuting flights and much longer trans-oceanic flights over the ocean where nothing obscures the wind stream. Recent tracking studies of these seabirds reported that large-scale trans-oceanic movements were shaped by large-scale global wind patterns (Egevang et al., 2010; Shaffer et al., 2006; Weimerskirch et al., 2015). Compared to the large-scale global wind patterns, the local wind patterns vary from hour to hour, where low and high-pressure systems pass continuously. These atmospheric pressure systems sometimes cause no wind in doldrums and occasionally strong winds associated with storms, which both could cause a significant effect to their movement (Catry et al., 2004; Weimerskirch et al., 2016). Seabirds should be able to react adequately to such fine-scale variation of winds to save time and energy consumption (Hedenström et al., 2002; Liechti, 2006). Therefore, revealing the bird's flight behavior to cope with such local wind patterns is a key to understand the movement strategy and the resulting energy budgets of the birds.

The development of bio-logging devices enabled to record flight behavior of the birds in the scale of seconds (Amélineau et al., 2014; Gibb et al., 2017; Sachs et al., 2013; Shimatani et al., 2012; Spivey et al., 2014; Treep et al., 2015). However, the local fine-scale observations of wind relevant to the scale of these birds' flight behavior lack due to spatially and temporally coarse measurement of ocean wind by conventional methods, such as satellites, buoys, balloons, and weather stations.

Moreover, the coarse wind information is not precisely the wind that is experienced by the birds both horizontally and vertically, because buoys and weather stations are often displaced from the bird's position in a kilometer scale, and satellite-based wind observations are fixed at 10 m reference height. Therefore, fine-scale wind observation that is temporally and spatially relevant to the seabird's movement is a key to address the seabird's movement strategy with the wind.

Fine-scale wind information in the context of meteorological observations

Recently, remote sensing systems used to record atmospheric circulation have been developed. Satellite-borne scatterometers estimate ocean surface wind velocities each day which covers a wide range of the global ocean (Fig. 2-1). These wide-range satellite-based wind data in combination with refined ocean-atmosphere models are utilized in numerical weather predictions and to describe the oceanographic features (Chelton et al., 2004; Chelton et al., 2006; Liu, 2002). Buoys scattered over the ocean measure high time resolution surface winds. These in situ observations of wind are used to validate remote sensing wind measurements and are assimilated into meteorological model analyses (Ebuchi et al., 2002; Pickett et al., 2003). However, since wind data is only acquired twice per day by each satellite with many unobserved gaps (Fig. 2-1), and buoys have limited spatial coverage, fine-scale changes of hours to days in local wind conditions might be overlooked. Also, wind data are lacking in coastal areas due to interference caused by complex topographic effects which makes satellite-based wind measurements obscure (Albert et al., 2010; He et al., 2004; Pickett et al., 2003). Obtaining in situ high resolution atmospheric and oceanographic data to fill these spatial and temporal observation gaps would deepen our understanding of physical processes relevant to interactions between the atmosphere and ocean. It is expected to improve atmospheric and ocean model analyses (Albert et al., 2010; He et al., 2004), and reveal detailed structure which remains unresolved by using only remote-sensing methods (Kawai et al., 2015).

The recent development of miniaturized animal-borne data loggers presented a unique

capability to use animals as indicators of environmental variables. The extensive movement range and locomotion ability of marine mammals and seabirds enabled environmental observations to be obtained in places and scales unresolved by conventional methods. For example, instrumented seals have been providing temperature and salinity profiles in the Antarctic Ocean for more than ten years, especially under sea-ice coverage which was impossible to measure by satellites (Biuw et al., 2007; Charrassin et al., 2008). Bird-borne sensors are also utilized in measuring environmental variables such as temperature, depth and light intensity directly from the instruments carried by the animal (Charrassin et al., 2002; Durant et al., 2009; Weimerskirch et al., 1995; Wilson et al., 2002). Besides direct measurement from animal-borne instruments, indirect evaluation of flow velocity can be made particularly when the animal's movements are passively driven or strongly affected by the flow. Studies have evaluated velocity of air and water flows from bird movement trajectories which are the consequence of bird movement itself and the drift caused by the flow. For example, wind velocity and the state of a bird in relation to the wind can be evaluated using statistical models (Shimatani et al., 2012). Three-dimensional flight paths of thermal soaring raptors have been used to estimate the horizontal and vertical component of wind in the mountain regions which agreed with measurements from meteorological stations (Treep et al., 2015). Furthermore, movements of shearwaters floating on the ocean surface were used to derive high-resolution ocean surface currents which matched in situ and remote sensing measurements of currents (Yoda et al., 2014). These studies demonstrate the potential of free-ranging animals as an indicator of environmental information.

Study objectives

Wind information in the scale of tens of minutes is essential from the perspective of movement ecology of seabirds and meteorological observations. This chapter aims to propose a simple method to estimate wind velocity from a bird's trajectory. First, global positioning system (GPS) units were deployed on the backs of three species of soaring seabirds, streaked shearwater (*Calonectris*

leucomelas), Laysan albatross (*Phoebastria immutabilis*), and wandering albatross (*Diomedea exulans*) to investigate fine-scale flight trajectories. Then, wind velocities were estimated from the flight trajectories of the birds, taking advantage of the ground speed change caused by wind resistance and assistance. The accuracy of the bird-based wind estimations is examined, and possible effects of a bird's flight strategy to the wind estimation are discussed. The use of the estimated wind to reveal the ecological and bio-mechanical aspect of bird flight is further discussed in chapter 3. The contribution of the estimated wind to meteorology by using soaring seabirds as "living ocean buoys" is suggested in chapter 4.

Materials and Methods

Field Experiments

In this study, data from three species of Procellariiformes were used: streaked shearwater (mean body mass 0.6 kg), Laysan albatross (3.1 kg), and wandering albatross (9.7 kg). GPS loggers used in the field studies were GiPSy-2 (Technosmart, Rome, Italy) for streaked shearwaters and Laysan albatrosses, and GPL20 (Little Leonardo, Tokyo, Japan) for wandering albatrosses. GiPSy-2 was powered by a Li-$SOCl_2$ battery, and wrapped by heat shrink tube for waterproof. The mass of the loggers was approximately 25 g (GiPSy-2) and 80 g (GPL20), which was less than 5% of bird's body mass. GPS loggers were attached to the back of the birds with waterproof tape (Tesa, Hamburg, Germany) and they were retrieved after the birds returned to their nests. GPS loggers were set to take one positional fix every second.

GPS loggers were attached to eight and nine streaked shearwaters simultaneously on August 29th and September 2nd, 2014, respectively, at a breeding colony of the Funakoshi-Ohshima Island (39°24'N, 141°59'E) in Japan. At this study site, more than 100 nests are marked for research and individuals are identified by the ring attached to the tarsus. Adult birds returning to their nests to feed their chicks were easily caught by hand through the entrance or a small hole dug on the top of the

burrows. One bird lost its instrument before recapture, and another bird was not recaptured. Thus, seven and eight loggers were retrieved, respectively. Two of the retrieved loggers did not record enough data. The remaining seven and six datasets were used in further analysis. The procedures of the field study were approved by the Animal Experimental Committee of The University of Tokyo, and this work was conducted with permission from the Board of Education of Iwate prefecture and the Coastal Wide-Area Promotion Bureau of Iwate prefecture, Japan.

The field study of Laysan albatross was conducted in February 2014 at the Ka'ena Point, Oahu Island breeding colony (21°34'N, 158°16'W) in Hawaii. GPS loggers were attached to three birds, and all were recaptured. One logger did not record enough data, so the remaining two datasets were used in further analysis. The experiment was conducted under permission from the Hawai'i Department of Land & Natural Resources and the United States Geological Survey Bird Banding Laboratory.

The field study of wandering albatross was conducted in March 2007 at Possession Island, Crozet archipelago (46°25'S, 51°44'E) in South Indian Ocean by Katsufumi Sato (Atmosphere and Ocean Research Institute, The University of Tokyo). GPS loggers were attached to six birds, and all were recaptured. Two loggers failed to record due to exposure to seawater, and the remaining four datasets were used in further analysis. The experiment was conducted under permission from the ethics committee of the Institute Polaire Paul Emile Victor, France.

Initial processing of GPS data

The raw data downloaded from GPS loggers included gaps; missing data of one to few seconds, and overlaps; continuous data assigned to the same time-stamp. Although the number of gaps and overlaps were much smaller than the total data length, the gaps were interpolated, and overlaps were deleted to make a continuous data with an equal time interval. Cubic spline was used to interpolate the gaps of longitude and latitude. When multiple data points were assigned to the same

time, the data point appeared first was kept and other data points were deleted to prevent equal time interval.

Speed and direction

Movement speed and direction of the birds were derived from the GPS positional data (Fig. 2-2A). The ground speed of the bird at each position ($P_i(x_i, y_i)$) was defined by the distance between consecutive positions (P_i) and (P_{i+1}) divided by the time interval; 1 second (Fig. 2-2A). Flight direction of the bird at each position (P_i) was defined by the anti-clockwise angle between east and the direction of the line connecting consecutive positions (P_i) and (P_{i+1}) (Fig. 2-2A). This direction corresponds to the ground velocity of the bird, not the heading that corresponds to the air velocity of the bird. The GPS units used in this study continuously communicated with the satellites to obtain one fix per second which sustained high relative accuracy between consecutive positional fixes. However erroneous GPS positions were obtained infrequently. Speed and direction data corresponding to these erroneous GPS positions were eliminated by using the speed data; points accompanied by ground speed over 50 ms^{-1} were excluded and replaced by linear interpolation.

Extract flight phase

The trajectory was divided into two phases: resting and flight, based on the ground speed of the bird. The histogram of ground speed was bimodal (Fig. 2-3). The peak at lower ground speed corresponds to resting on sea surface or land, and the peak at higher ground speed corresponds to flight (Shiomi et al., 2012; Weimerskirch et al., 2002). These two behavioral phases can be divided at a ground speed of approximately 4 ms^{-1} based on the bimodal histogram (Fig. 2-3). Streaked shearwaters frequently showed cyclic flight maneuvers — repeating flight against the wind and following the wind in a few seconds scale. The flight against the wind in this cycle occasionally caused few seconds of low ground speed under 4 ms^{-1}, so simply dividing rest and flight behaviors

based on 4 ms^{-1} ground speed threshold caused spurious resting phases during cyclic flight maneuvers. Therefore, resting phases were defined as where low ground speed under 4 ms^{-1} was kept for at least 5 seconds. The rest of the track was assigned to flight phase.

Estimate wind velocity from the trajectory of bird flight

Ground velocity is the sum of air velocity and wind velocity. When there is no wind, ground velocity is identical to the air velocity in any heading directions. When there is wind, however, ground speed increases in a tailwind, decreases in a headwind, and shows an intermediate value in a sidewind, according to the amount of assistance or resistance from the wind. Therefore, the ground speed changes in a continuous manner in relation to flight direction due to the effect of wind. Maximum ground speed should be achieved in pure tailwind which equals the sum of airspeed and wind speed, whereas minimum ground speed should be achieved in pure headwind which equals wind speed subtracted from airspeed. Here, the relationship between flight direction and ground speed was used to estimate air velocity and wind velocity by fitting a cosine curve or a circle (Fig. 2-2B, C).

The relation between flight direction and ground speed can be approximated by a cosine curve (Shimatani et al., 2012). A cosine curve was fitted to the relation between ground speed and flight direction using the following equation:

$$V_g = V_w \cos(\theta - \theta_w) + V_a \quad (2\text{-}1)$$

Maximum likelihood estimates of wind speed (V_w), wind direction (θ_w), and airspeed (V_a) could be obtained by using the observed series of ground speed (V_g) and flight direction (θ), assuming a Gaussian distribution for ground speed (V_g). Wind speed (V_w) could be graphically shown as the one-half of the difference between the maximum and the minimum ground speed obtained from the fitted cosine curve (Fig. 2-2B). Wind direction (θ_w) could be graphically shown as the direction where the maximum ground speed is achieved (Fig. 2-2B).

The relation between air, ground, and wind vectors were precisely expressed by fitting a circle to the ground velocity vector by minimizing the following equation, which is the sum of squared difference between the data points and the closest point on the circle (Fig. 2-2C).

$$\sum \left\{ \sqrt{\left(V_g \cos\theta - V_w \cos\theta_w\right)^2 + \left(V_g \sin\theta - V_w \sin\theta_w\right)^2} - V_a \right\}^2 \quad (2\text{-}2)$$

Wind speed (V_w), wind direction (θ_w), and airspeed (V_a) can be estimated from this equation using the observed series of ground speed (V_g) and flight direction (θ) (Fig. 2-2C). The estimated wind vector can be graphically shown as the vector from the origin to the center of the fitted circle (Fig. 2-2C). The estimated airspeed can be graphically shown as the radius of the fitted circle (Fig. 2-2C). Cosine fitting and circle fitting methods were compared where satellite-based winds were available for verification.

Apply two-dimensional wind estimation to bird trajectory

Only the flight phases lasting longer than 10 minutes were used in the wind estimating analysis. One minute after take-off and one minute before landing were excluded from the analysis considering the effect of frequent flapping accompanied with rapid acceleration and deceleration which could differ from the cruising speed (Kogure et al., 2016; Sato et al., 2009). Each flight phase was divided into series of 5-minutes windows (Fig. 2-2A). This 5-minutes section length was a consequence of a trade-off between the need for sufficient numbers of data points to estimate wind while keeping a high temporal resolution. It is also comparable to 5-minutes to a 1-hour interval of the in-situ measurements from buoys and weather stations for further validation. Cosine fitting was applied to each section to estimate wind velocity. Mean latitude and longitude of each section were calculated to represent the positions of the estimated wind. Circular deviance of each flight section was calculated to represent the variation of flight direction. To avoid ambiguous estimation of wind direction Akaike's information criterion (AIC) was calculated for cosine curve fitting (AIC_{cos}) and

line fitting with a fixed slope of zero (AIC_{null}) in each section, assuming normal distribution around each fitting. The wind was not estimated when $AIC_{cos} > AIC_{null} - 2$. This selection of fitting avoided wind velocity estimation when the variation of flight direction was small, or the ground speed variation seemed random, not reflecting the effect of wind velocity. It also avoided wind estimation when wind speed was extremely weak.

Validation of two-dimensional bird-based wind estimates by satellite-based wind measurements

The bird-based wind speed and direction were compared with wind estimated by satellite-borne scatterometers to examine the accuracy. The scatterometers transmit microwave pulses to the ocean surface and measure the surface roughness from the backscattered pulses. Wind speed and direction are estimated by relating the surface roughness to wind stress. The satellites orbit the earth twice per day and estimate wind speed and direction in continuous swaths covering large parts of the global ocean (Fig. 2-1). The reference wind speed and direction data were obtained from the SeaWinds microwave scatterometer instrument flown on the QuikSCAT spacecraft (QSCAT) and the Advanced Scatterometer instrument flown on the EUMETSAT MetOp-A satellite (ASCAT) from Physical Oceanography Distributed Active Archive Center (PODAAC, http://podaac.jpl.nasa.gov/). Wind speed and direction data were downloaded from OPeNDAP in PODAAC where wind velocities were gridded in 12.5 × 12.5 km resolution in 10 m reference height for both QSCAT and ASCAT. Wind speed and direction from QSCAT was used for comparison with 2007 dataset (wandering albatross) and ASCAT for 2014 dataset (streaked shearwater and Laysan albatross). Bird-based winds and satellite-based winds were collocated for comparison by choosing the nearest point both temporally and spatially. Temporal difference and spatial separation were limited to 2 hours and 10 km — within the range of previous studies validating or comparing in-situ wind measurements with satellite-based winds (Adams and Flora, 2009; Freilich and Dunbar, 1999) — resulting in a maximum difference of

89 minutes and 8.6 km. In many cases, the location of the bird-based wind data was between the swaths of satellite-based wind measurements which caused large spatial separation. Twelve out of 20 compared points were from different individuals (all points from shearwaters are from different individuals), and a maximum of four points are obtained from the same individual (wandering albatross). Comparison points from the same individual were temporally separated by at least 12 hours which could be treated as temporally independent observations. Due to the small amount of collocated data between bird-based and satellite-based wind estimates, here the wind estimates from all species were pooled to validate the bird-based wind using satellite-based wind estimates statistically.

Wind speed and direction estimated by both the cosine fitting and the circle fitting methods were compared with satellite-based wind estimates. Bird-based wind velocities and satellite-based wind velocities were both decomposed to x and y components in earth-oriented Cartesian coordinates, x increases along the eastward axis and y increases along the northward axis. The generalized vector correlation coefficient was calculated to evaluate the degree of correlation between bird-based and satellite-based wind velocities (Crosby et al., 1993). This coefficient takes into account both wind speed and direction and shows a value between 0 and 2, 0 indicating no correlation and 2 indicating a complete correlation between two series of vectors.

The generalized vector correlation coefficient is independent of the scaling effect to vector datasets by either a constant magnitude or angular shift. Therefore, the wind speeds and the directions of satellite-based and bird-based winds were further compared separately. Wind speeds were compared by applying Passing-Bablok regression (Passing and Bablok, 1983) using mcreg function in mcr package in R ver. 3.0.0. Although the satellite-based wind estimates used as the reference data for validation also include error, Passing-Bablok regression compares two different methods (bird-based and satellite-based) estimating the same parameter (wind speed) taking into account that both of the estimating methods have an error. Wind directions of satellite-based and bird-based wind estimates were compared by the Fisher-Lee parametric test for angular correlation (Zar, 1999) to test whether

there was a correlation between them. All the analyses in the method section were done using Igor Pro (WaveMetrics) with the advanced add-on "Ethographer", MATLAB (MathWorks), and R (R Core Team).

Results

Wind estimates from the flight trajectories of soaring seabirds

A total of 353, 74, and 185 hours of positional data were obtained from streaked shearwaters (27.2 ± 12.9 hours, n = 13), Laysan albatrosses (37.1 ± 4.0 hours, n = 2), and wandering albatrosses (46.3 ± 1.2 hours, n = 4), respectively. A total of 1685, 718, and 744 sections of wind estimates were obtained from each species. The number of sections in which wind estimation was avoided by the model selection based on AIC was 21 (1.2%) for streaked shearwaters, 18 (2.5%) for Laysan albatrosses, and 5 (0.7%) for wandering albatrosses. Excluding these points resulted in 1664 wind data obtained from streaked shearwaters, 700 from Laysan albatrosses, and 739 from wandering albatrosses.

Extensive travel distances and prolonged flight durations of soaring seabirds enabled wide range estimation of wind speed and direction in fine-scale resolution. Estimated wind speed from streaked shearwater's trajectories ranged from 0.4 to 11.2 ms^{-1} with average of 3.4 ± 1.6 ms^{-1}. Data points were widespread in the ocean between Hokkaido and Sanriku in north-eastern Japan, and were densely distributed mainly near the Sanriku coast (ca. <100 km from land) (Fig. 2-4) because the birds frequently returned to their colony at the coastal island to feed their chick. Offshore winds estimated by long-distance foraging trips (ca. 500 km) were relatively strong while speeds of coastal winds estimated by short distance foraging trips (ca. < 100 km) were weaker and changed direction frequently (Fig. 2-4).

Laysan albatrosses' flight extended to the northern ocean of Hawaii islands with a total of 718 bird-based wind estimates from two birds (Fig. 2-5). During the northward flight, both the

bird-based wind estimates and the satellite-based wind measurement showed a weak wind (ca. < 1 ms^{-1}) indicating that a high-pressure system might have passed this region (Fig. 2-5).

Wandering albatrosses' flight was recorded in a wide area of the Southern Indian ocean with a total of 744 bird-based wind estimates from four birds (Fig. 2-6). The average wind speed of the bird-based winds was stronger compared to the other two species reflecting that wandering albatrosses fly in a region where strong wind is dominant; the roaring forties. However, continuous change in wind speed was observed by the bird-based wind estimates indicating that the wind in roaring forties is not always consistent. One bird experienced weak winds in a northwestern travel (Fig. 2-6, ca. 43° S50° E) and one bird seemed to be trapped in the high-pressure cell (Fig. 2-6, ca. 46°S43°E).

Bird-based wind covered spatial and temporal observation gaps of conventional methods

The fine-scale time series of wind in the Sanriku coastal area estimated from the flight trajectories of 13 streaked shearwaters were further examined in the context of complementing satellite-based wind observations. Fine-scale resolution of the bird-based wind estimates covered temporal and spatial gaps between the remote sensing measurements. Each of the bird-based wind velocity represented the wind experienced by the birds during five-minute flights of approximately 2–3 km distance traveled. This resolution was higher compared to more than 12 hours and 12.5 km resolution of satellite-based wind observations. Dense spatial distribution of bird-based winds in coastal areas covered a key region where satellite-based wind measurements are lacking due to topographic effects (Fig. 2-4 and Fig. 2-7B, C). In addition, the high temporal resolution of the bird-based winds detected the dynamic change in wind direction from northerly winds to southerly winds that occurred between 0:00 to 12:00 UTC of September 3rd with timing differing according to the location of the birds (Fig. 2-7A). These changes were not recorded by the scatterometer wind estimation at 0:00 UTC Sep 3rd and 11:00 UTC Sep 4th, which is 35 hours apart, because of the coarse temporal resolution (Fig. 2-7B, C).

Verification of bird-based wind estimates

To examine the accuracy of the bird-based wind velocities, it was compared with the satellite-based wind velocities estimated by the QuikSCAT and ASCAT satellite scatterometers. Many of the bird-based wind measurements were located between the swaths or time regions of the satellite coverage (Fig. 2-1) resulting in a total of 20 collocated comparable points between bird-based and satellite-based winds (streaked shearwaters $N = 9$ (Fig. 2-4 and 2-8), Laysan albatrosses $N = 2$ (Fig. 2-5 and 2-9), and wandering albatrosses $N = 9$ (Fig. 2-6 and 2-10)). The generalized vector correlation coefficient (Crosby et al., 1993) that accounts for the correlation between two sets of vectors (lengths and directions) was used to compare the bird-based and satellite-based wind estimates. A significant correlation was shown between the bird-based and the satellite-based wind estimates both in cosine fitting ($\rho_v{}^2 = 1.66$, $P < 0.01$) and in circle fitting ($\rho_v{}^2 = 1.55$, $P < 0.01$).

In addition, wind speed and direction were validated separately. The bird-based wind speed was strongly correlated with the satellite-based wind speed for both the cosine fitting method (Fig. 2-11A, Pearson's $R = 0.93$, $P < 0.01$) and the circle fitting method (Fig. 2-11C, Pearson's $R = 0.83$, $P < 0.01$), but was underestimated. Comparison of wind direction between bird and satellite-based estimates showed good agreement for both the cosine fitting method (Fig. 2-11B, Angular correlation coefficient $R = 0.46$, $P < 0.01$) and the circle fitting method (Fig. 2-11D, Angular correlation coefficient $R = 0.52$, $P < 0.01$). The absolute difference between bird-based and satellite-based measurements of wind direction became larger in weak winds, particularly at some points from streaked shearwaters and a Laysan albatross (Fig. 2-12).

Discussion

Soaring seabirds are characterized by its unique dynamic soaring flight, which relies on the energy extracted from wind (Sachs, 2005; Sachs et al., 2013; Spivey et al., 2014). This flight strategy

provides two technical advantage of using soaring seabirds as an indicator of wind. First, the high ratio of gliding in soaring seabirds indicates that their movements are dominated by the effect of the wind. This suggests that the movement could be adequately modeled by a simple relationship between ground vector, air vector, and wind vector. Second, flight paths of shearwaters and albatrosses recorded in this study showed a tortuous pattern of dynamic soaring in fine-scale movement on the order of several tens of meters (Fig. 2-2A) which was associated with a fluctuation of ground speed and flight direction (Fig. 2-2B, C). This fluctuation provided sufficient variation of flight direction in a short period that enabled a successful fitting of a cosine curve or a circle, even when the bird seemed to fly in a certain direction over a large scale (Fig. 2-2A).

Wind velocities obtained from cosine curve and circle fitting methods both showed good agreement with the satellite-based wind velocities. This suggests that while circle precisely expresses the relationship between air, ground, and wind vector, cosine curve could be a good approximation. Circle fitting has an advantage that it directly treats the parameters as vectors. Cosine curve fitting has an advantage in its simplicity so that it could be expanded to model the movement of the birds by incorporating additional parameters into the function (Shimatani et al., 2012). Good agreement of the validation indicates that cosine curve fitting and circle fitting method are both valid for further application.

The bird-based estimates of wind velocities agreed well with the satellite-based wind measurements. This was in the range of vector correlation coefficients shown in studies that validate winds measured by satellite scatterometers with winds measured in situ by meteorological buoys (Adams and Flora, 2009; Freilich and Dunbar, 1999) ($\rho_v{}^2$ = 1.28 to 1.90). Comparison of wind direction between bird and satellite-based estimates showed good agreement. However, the absolute difference between bird-based and satellite-based measurements of wind direction became larger in weak winds, particularly at some points from streaked shearwaters and a Laysan albatross (Fig. 2-12). Studies that validate satellite-based wind estimates using the in-situ measurements by buoys also shows

that discrepancy in wind direction increases at weak winds (Adams and Flora, 2009; Freilich and Dunbar, 1999). Deviation from the true wind direction is crucial in strong winds but minor in weak winds; an extreme case is that wind direction has no information when wind speed is zero. This issue is addressed by calculating the vector correlation coefficient considering both speeds and directions (Crosby et al., 1993), which showed good agreement between the two methods. Scatterometers evaluate ocean surface wind velocities by measuring the ocean surface roughness. In coastal areas, the accuracy of satellite wind measurements decreases because of the complex wave structure and small-scale wind variation caused by topography. Validation of satellite-based winds using buoys-based wind measurements shows that mismatches occur most often near the shore (Adams and Flora, 2009; Freilich and Dunbar, 1999). This limited accuracy and difficulty in capturing small-scale wind variation at coastal areas might also explain the deviation of wind direction between the two methods, especially in shearwaters flying in such areas. On the other hand, wind directions estimated from flight paths of wandering albatrosses showed the strongest agreement with satellite-based wind directions (Fig. 2-11B, D) because this species flew far away from land in regions of strong persistent winds; the roaring forties (Fig. 2-5).

The bird-based wind speed was strongly correlated with the satellite-based wind speed but was underestimated (Fig. 2-11A, C); which has several possible explanations. First, satellite-based wind speed is extrapolated to a 10 m reference height while average flight height of studied birds is known to be below 10 m; approximately 2 m for shearwaters and 3–8 m for albatrosses (Pennycuick, 1982). This difference in height is suspected to be one of the causes of the underestimation of bird-based wind speed due to the wind shear where wind speed decreases near the ocean surface. To evaluate the discrepancy of wind speed due to the height difference, the logarithmic wind profile near the ocean surface was used (Stull, 2003) which showed that the corresponding flight height would be lower than 1 m to satisfy the underestimation of bird-based wind speed estimates. This indicates that the wind shear does not solely explain the discrepancy between bird and satellite-based wind speed estimates or that the logarithmic

profile was inappropriate to represent the experienced wind shear (Bousquet et al., 2017). Second, potential sources of error which might be related to the characteristics of soaring flight of the seabirds should be considered. The unique dynamic soaring flight pattern used by shearwaters and albatrosses does not only zigzags in the horizontal direction but also fluctuates in the vertical direction (Sachs et al., 2012; Sachs et al., 2013; Spivey et al., 2014). Therefore, the variation in ground speed includes the decrease and increase of ground speed associated with the gain and loss of altitude. Altitude variation related to the maneuvering of soaring birds consists of ascending against the winds and descending following the winds (Sachs, 2005; Sachs et al., 2013). This may cause the estimated wind speed to deviate from the true wind speed experienced by the bird. However, studies of dynamic soaring flight shows that potential energy associated with flight altitude is much smaller than the kinetic energy associated with fluctuating ground speed, indicating that wind resistance and assistance dominates ground speed fluctuation (Gibb et al., 2017; Sachs et al., 2012; Sachs et al., 2013). Another error can be caused by albatrosses and shearwaters that adjust their airspeed in relation to headwinds and tailwinds, with airspeed increasing in headwinds (Pennycuick, 1982; Spear and Ainley, 1997), because here an assumption was made that the bird flew in a constant airspeed in each section. However, airspeed adjustment is not relevant to the few seconds scale of the cyclic maneuver of dynamic soaring, and it is rather adjusted in a more larger scale relationship between wind direction and the bird's flight direction, which is discussed in chapter three. Although flapping effort, which increases with decreasing body size (Sato et al., 2009), might also affect wind speed estimation especially in relatively small-sized shearwaters, this should have small effect because intermittent flapping of soaring seabirds is considered to keep air speed in a certain range for sustainable flight (Pennycuick, 1987; Spivey et al., 2014), and take-offs and landings associated with rapid increase or decrease in ground speed by flapping (Kogure et al., 2016; Sato et al., 2009) was excluded from the analysis. The strong correlation between bird-based and satellite-based wind speeds suggest that bird-based wind speeds could be converted to comparable values for practical use. Further analysis of the complex dynamics of the flight of these birds can

increase estimation accuracy, especially by recording flight height to determine the reference height of the estimated wind velocities.

Although indirect measurement from flight paths of soaring seabirds might include errors related to behavior and flight strategy of the birds, bird-based and satellite-based wind velocities were strongly correlated, suggesting that these estimated wind velocities have sufficient accuracy for further practical use in both the study of seabird's flight behavior and meteorological wind observations. Still, it is necessary to carefully address the estimation errors caused by flight behavior and the difference between species through validation, and further improve the accuracy by analysis of three-dimensional flight trajectories.

Table2-1. Information of the birds equipped with loggers.

Species	Logger attached (year/month/day)	Logger retrieved (year/month/day)	Body mass (kg)	Sex	Logger	Remarks
Streaked shearwater	2014/9/2					fell off
	2014/8/29	2014/9/3	0.62	M	Gipsy	
	2014/9/2	2014/9/3	0.58	M	Gipsy	
	2014/8/29	2014/8/30	0.56	F	Gipsy	
	2014/9/2	2014/9/3	0.67	M	Gipsy	
	2014/9/2	2014/9/6	0.50	F	Gipsy	
	2014/8/29	2014/9/1	0.60	M	Gipsy	
	2014/9/2	2014/9/5	0.50	F	Gipsy	insufficient data
	2014/9/2	2014/9/3	0.62	M	Gipsy	insufficient data
	2014/8/29	2014/8/30	0.63	M	Gipsy	
	2014/9/2	2014/9/9	0.60	M	Gipsy	
	2014/8/29					not recaptured
	2014/8/29	2014/8/30	0.49	F	Gipsy	
	2014/9/2	2014/9/5	0.46	F	Gipsy	
	2014/8/29	2014/9/1	0.60	M	Gipsy	
	2014/9/2	2014/9/3	0.62	M	Gipsy	
	2014/8/29	2014/9/1	0.59	M	Gipsy	
Laysan albatross	2014/2/3	2014/2/8	3.1	U	Gipsy	
	2014/2/4	2014/2/7	3.1	F	Gipsy	
Wandering albatross	2007/2/21	2007/3/3	7.2	F	GPL20	
	2007/3/6	2007/3/15	8.7	F	GPL20	
	2007/3/13	2007/3/27	11.3	M	GPL20	
	2007/3/17	2007/3/21	11.0	M	GPL20	

Species names, logger attached date, logger retrieved date, body mass, sex (M: male, F: female, U: unknown), logger name, and the reason for exclusion from the analysis are shown.

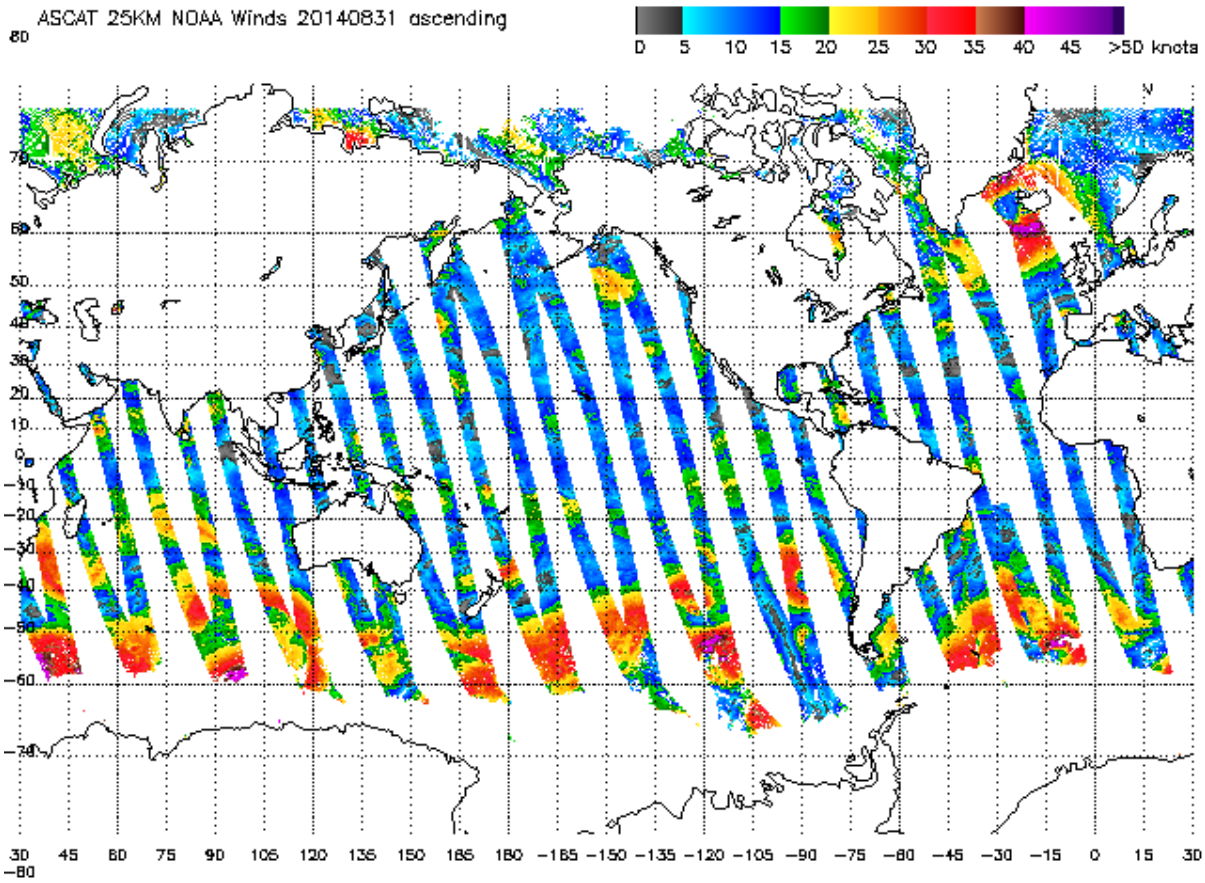

Fig. 2-1. An example of the swaths of wind measurements by the satellites.

The wind measurement from the ASCAT Metop-A (advanced scatterometer) in 31 August 2014 (ascending path). The satellite orbits around the earth to measure winds by microwave pulses. These swaths of wind measurements are obtained twice per day (ascending and descending paths), however, large gaps are left unobserved such as the east coast of Japan where experiments were conducted on this day. The figure is copied from the STAR (Center for Satellite Application and Research) webpage.

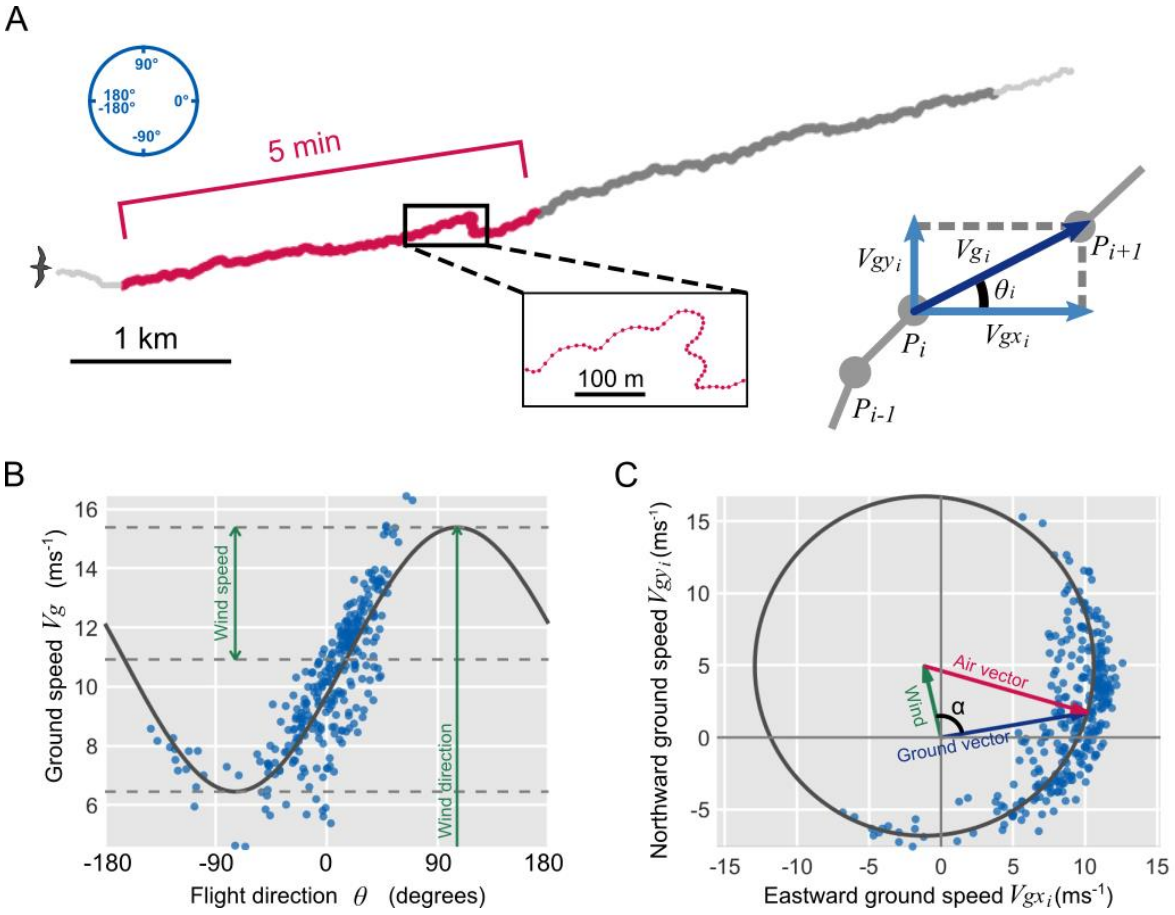

Fig. 2-2. Estimation of wind from the ground speed and direction of the birds.

(A) An example of a flight path of streaked shearwater obtained from GPS records. Flight is separated into 5-minutes sections (red part). Enlarged view of the flight path shows the zigzag dynamic soaring flight (bottom box). Flight direction (θ) and ground speed (V_g) (dark blue arrow) with eastward (V_{gx_i}) and northward (V_{gy_i}) component (light blue arrows) is defined for each position (P_i). Direction is zero towards east and positive anticlockwise (top left). **(B)** Cosine curve fitting to the relationship between flight direction and ground speed of the red section shown in (A). Wind speed is graphically shown as the half the difference between maximum and minimum values of the fitted curve (green two-way arrow). Wind direction is estimated as the direction where maximum value is obtained by the fitted circle (green one-way arrow). **(C)** Scatter plots of ground velocity and the fitted circle of the red flight section shown in (A). Wind velocity (green arrow), air velocity (red arrow), and ground velocity (blue arrow) are shown. Bird-wind angle (α) is defined as the angle between the ground vector and the wind vector.

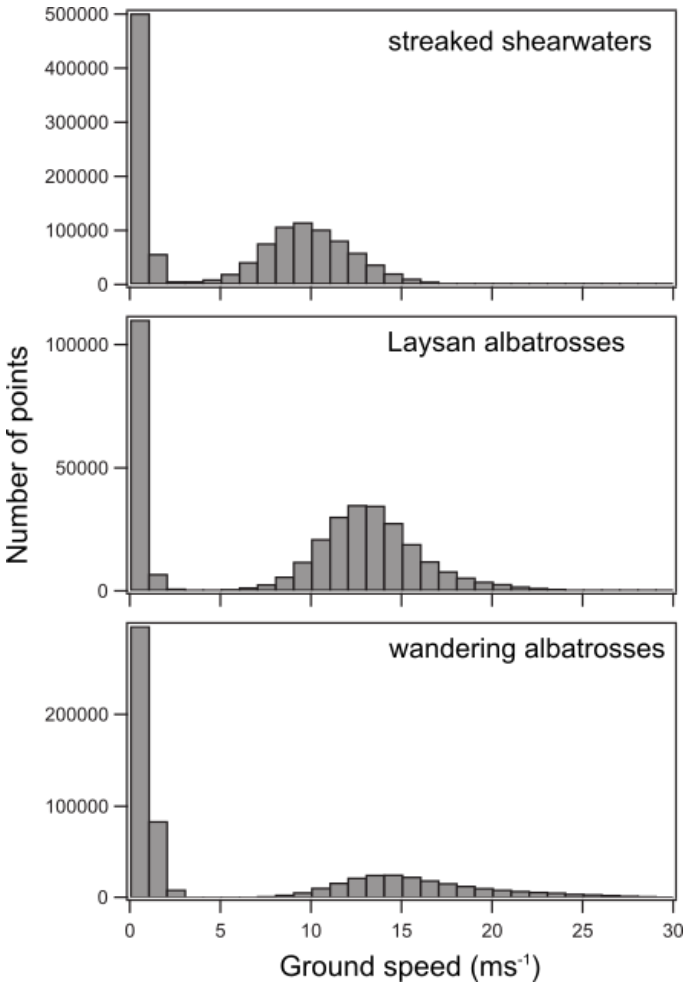

Fig. 2-3. Histograms of ground speed.

Histograms of the ground speed of streaked shearwaters (N = 13), Laysan albatrosses (N = 2), and wandering albatrosses (N = 4). All histograms show bimodal distribution where low speed corresponds to resting and high speed corresponds to flight. Ground speed of 4 ms^{-1} was set as the threshold to divide rest and flight phase.

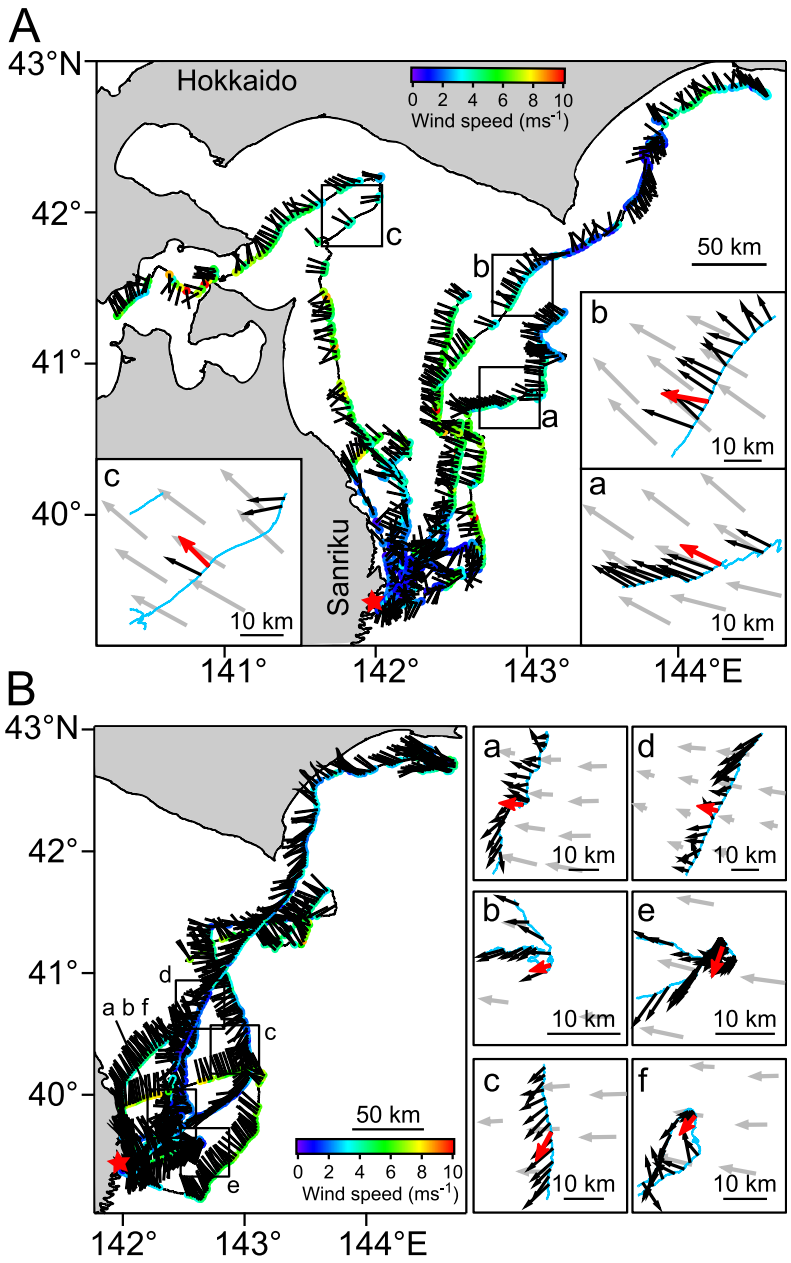

Fig. 2-4. Wind estimated from the flight of streaked shearwaters.

Bird-based winds are mapped on the flight paths of **(A)** seven streaked shearwaters released on August 29th, 2014 and **(B)** six streaked shearwaters released on September 2nd, 2014. Wind speed (colors) and direction in which the wind is blowing (black bars) is shown. Stars indicate the breeding colony. Points where bird-based wind was compared with satellite-based wind are shown in boxes. Estimated wind vectors (black arrows) are mapped on the bird's flight track (light blue lines). Satellite-based wind measurements are mapped (gray arrows). Bird-based winds temporally closest to the satellite-based wind measurements are shown (red arrows).

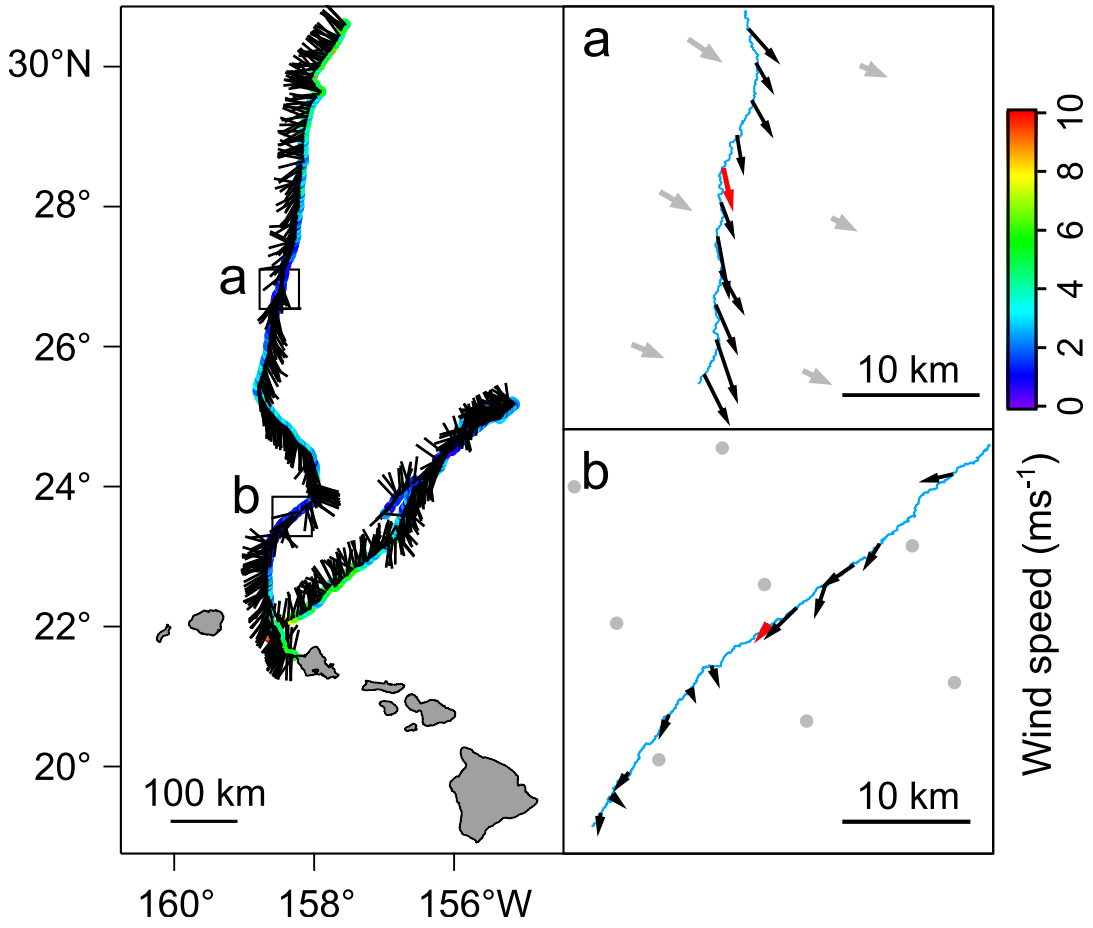

Fig. 2-5. Wind estimated from the flight of Laysan albatrosses.

Bird-based winds are mapped on the flight paths of two Laysan albatrosses. Wind speed (colors) and direction in which the wind is blowing (black bars) is shown. Points where bird-based wind was compared with satellite-based wind are shown in boxes. Estimated wind vectors (black arrows) are mapped on the bird's flight track (light blue lines). Satellite-based wind measurements are mapped (gray arrows). Extremely weak winds are shown in grey circles. Bird-based winds temporally closest to the satellite-based wind measurements are shown (red arrows).

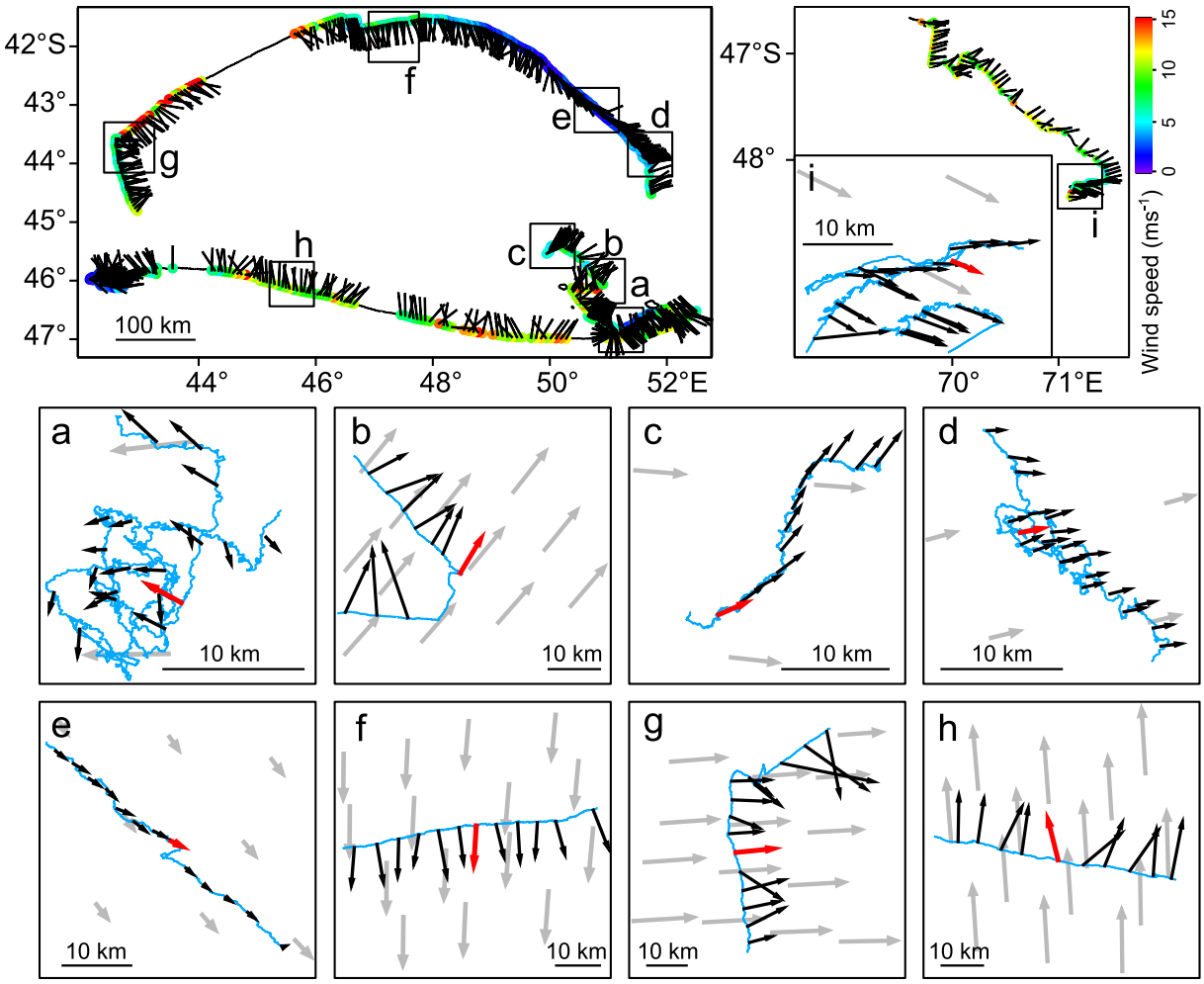

Fig. 2-6. Wind estimated from the flight of wandering albatrosses.

Bird-based winds are mapped on the flight paths of four wandering albatrosses. Wind speed (colors) and direction in which the wind is blowing (black bars) is shown. Points where bird-based wind was compared with satellite-based wind are shown in boxes. Estimated wind vectors (black arrows) are mapped on the bird's flight track (light blue lines). Satellite-based wind measurements are mapped (gray arrows). Bird-based wind temporally closest to the satellite-based winds measurements are shown (red arrows).

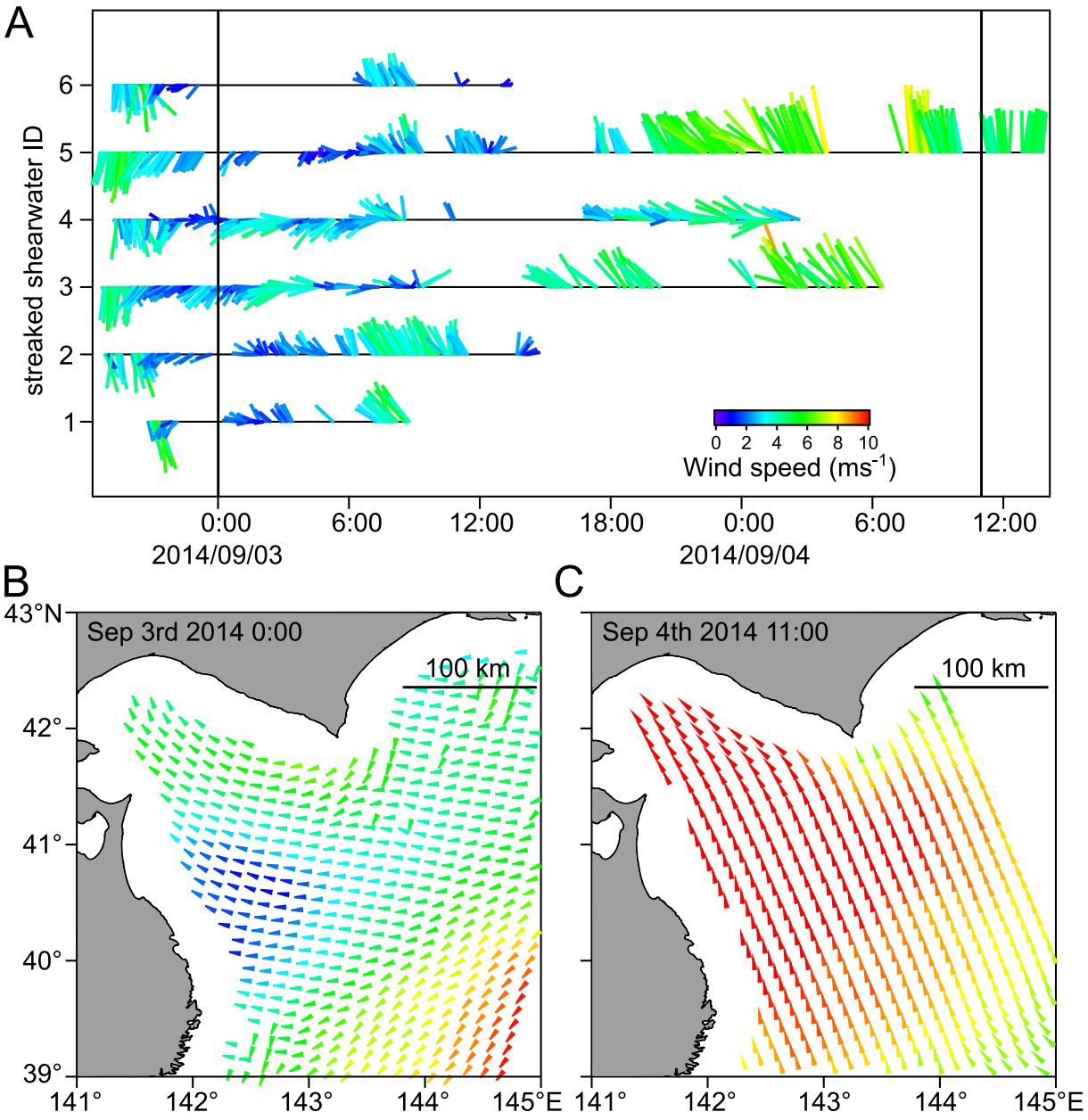

Fig. 2-7. Bird-based wind estimates covering the temporal gaps of satellite-based wind observations.

(A) Temporal view of the bird-based winds by six streaked shearwaters released on September 2nd, 2014. Two black vertical lines indicate the times when a satellite scatterometer estimated the wind in the sea of north-eastern Japan. **(B)** The satellite-based wind on approximately 0:00 UTC of September 3rd, 2014 and **(C)** 11:00 UTC of September 4th, 2014. There are data gaps at the coastal area and outside the measurement band.

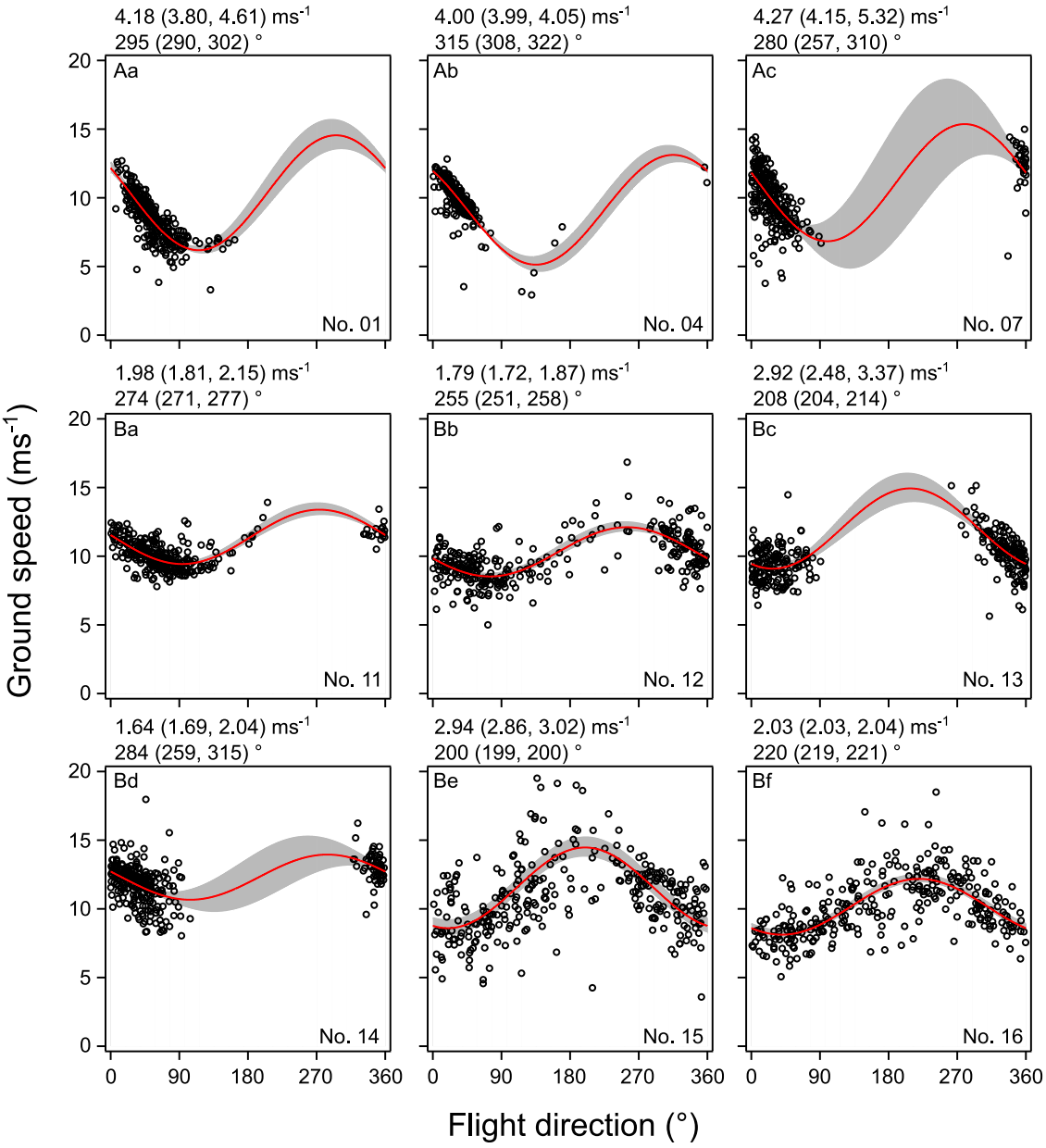

Fig. 2-8. Wind estimation by cosine curve fitting in streaked shearwaters.

Cosine curve fitting against the relationship between ground speed and direction in nine flight sections of streaked shearwaters where the bird-based wind estimates were compared with satellite-based wind estimates. Red curves are the fitted cosine curves. The 95% prediction intervals are shown in gray. Estimated wind speed and direction are shown above each box with lower and upper 95% confidence intervals in parentheses. The number on the right bottom of each box represents the individual number. Each box is linked to the comparison points shown in Fig. 2-4.

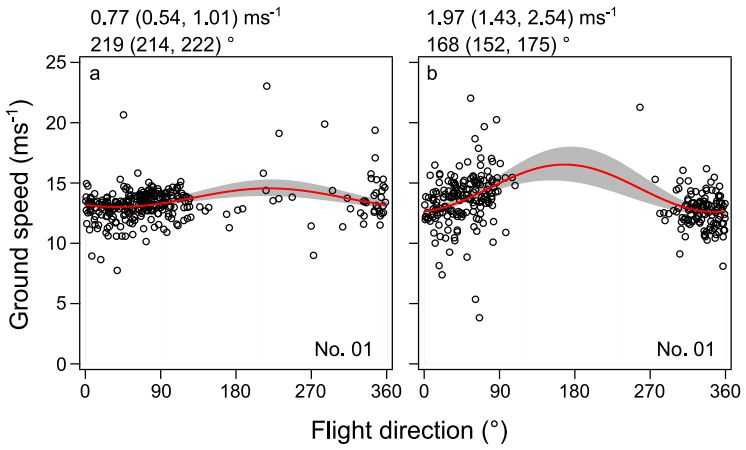

Fig. 2-9. Wind estimation by cosine curve fitting in Laysan albatrosses.

Cosine curve fitting against the relationship between ground speed and direction in two flight sections of Laysan albatrosses where the bird-based wind estimates were compared with satellite-based wind estimates. Red curves are the fitted cosine curves. The 95% prediction intervals are shown in gray. Estimated wind speed and direction are shown above each box with lower and upper 95% confidence intervals in parentheses. The number on the right bottom of each box represents the individual number. Each box is linked to the comparison points shown in Fig. 2-5.

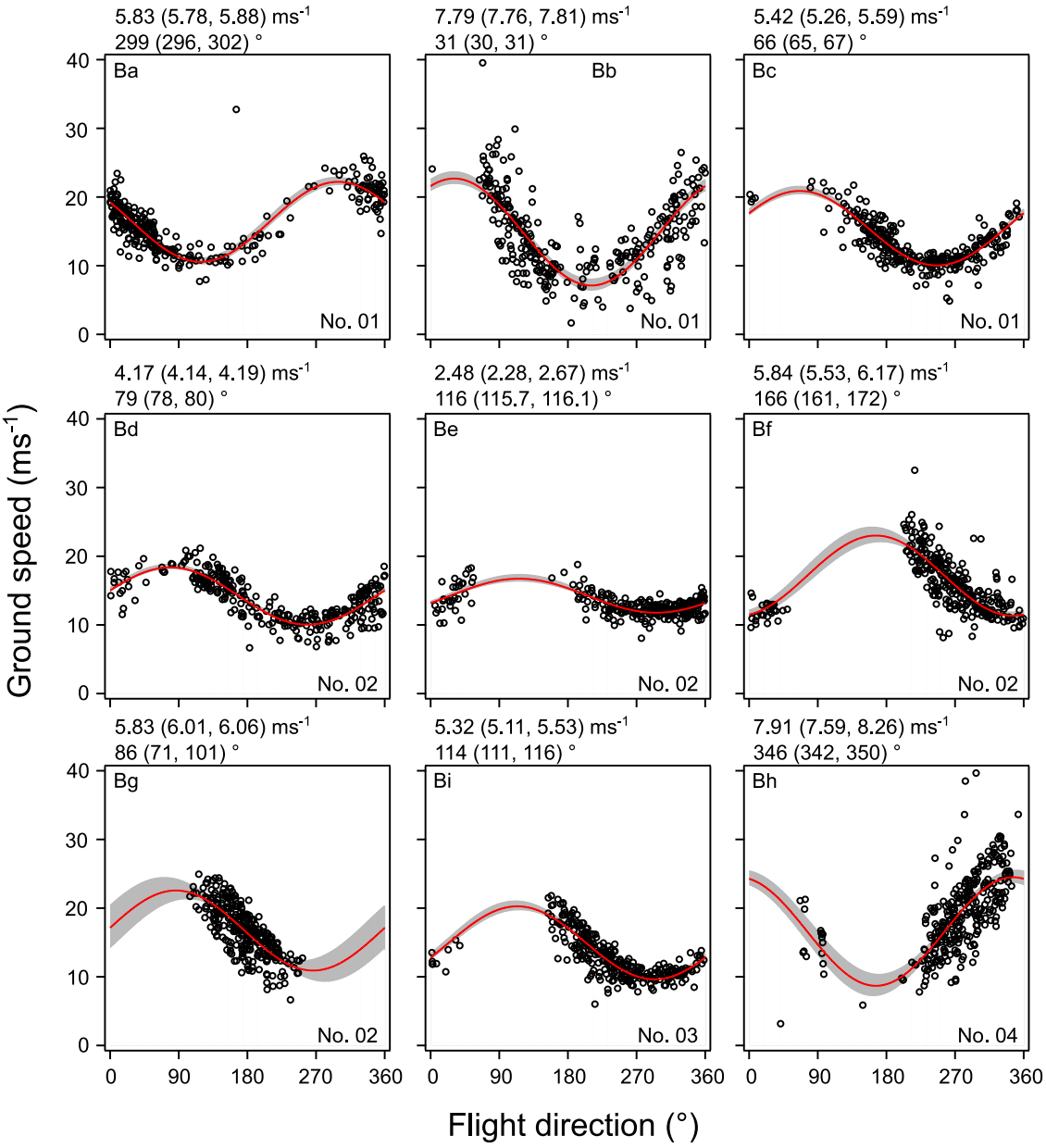

Fig. 2-10. Wind estimation by cosine curve fitting in wandering albatrosses.

Cosine curve fitting against the relationship between ground speed and direction in nine flight sections of wandering albatrosses where the bird-based wind estimates were compared with satellite-based wind estimates. Red curves are the fitted cosine curves. The 95% prediction intervals are shown in gray. Estimated wind speed and direction are shown above each box with lower and upper 95% confidence intervals in parentheses. The number on the right bottom of each box represents the individual number. Each box is linked to the comparison points shown in Fig. 2-6.

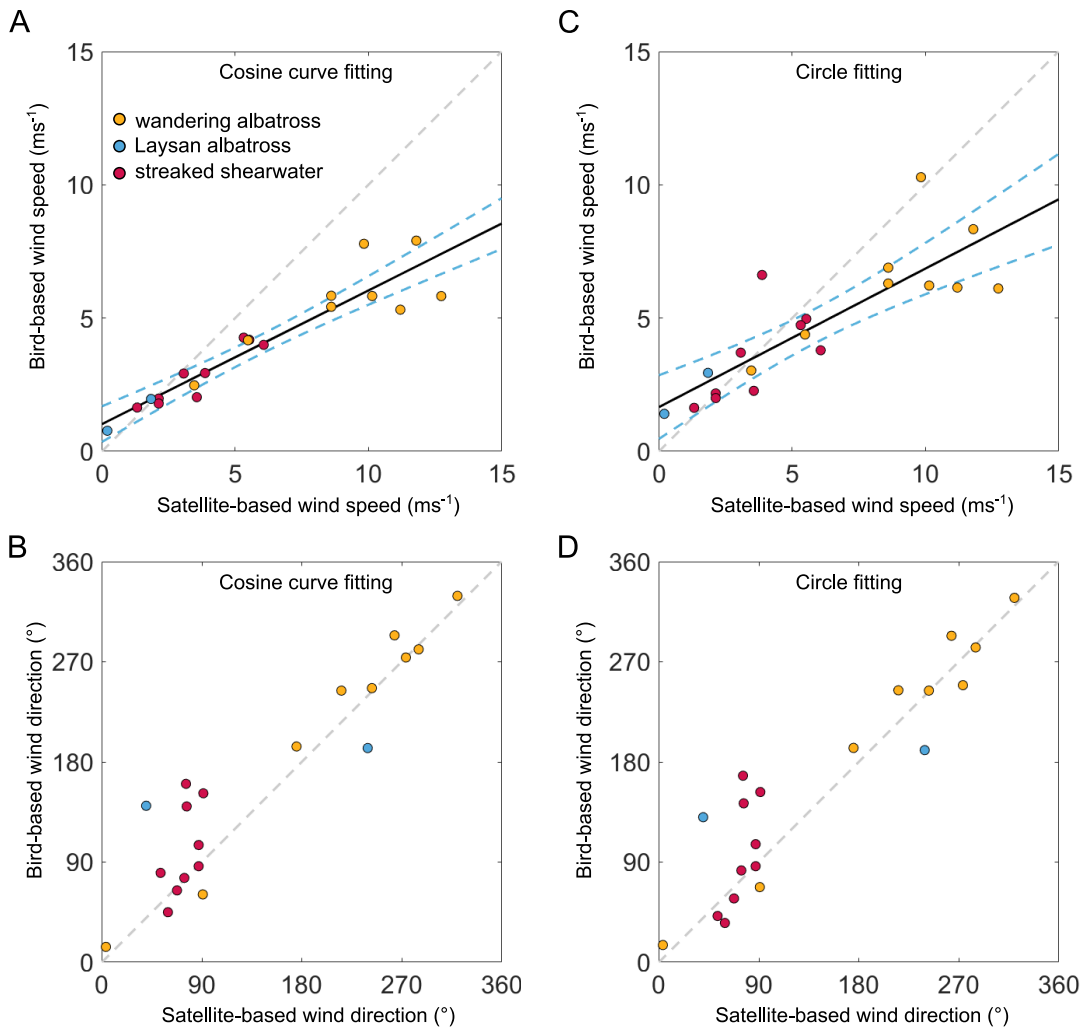

Fig. 2-11. Comparison between bird-based and satellite-based wind velocities.

(A, B) The relationship between bird-based (V_{bird}) and satellite-based (V_{sat}) wind speeds for **(A)** the cosine curve fitting method ($V_{bird} = 0.50V_{sat} - 1.02$, Pearson's $R = 0.93$, $P < 0.01$) and **(B)** the circle fitting method ($V_{bird} = 0.52V_{sat} - 1.66$, Pearson's $R = 0.83$, $P < 0.01$). Gray dashed line represents equal speed. Blue dashed line represents the 99% confidence intervals. **(C, D)** The relationship between bird-based and satellite-based wind directions for **(C)** the cosine curve fitting method (angular correlation $R = 0.44$, $P < 0.01$) and **(D)** the circle fitting method (angular correlation $R = 0.52$, $P < 0.01$). Gray dashed line represents equal directions. Color represents streaked shearwaters (red), Laysan albatrosses (blue), and wandering albatrosses (orange).

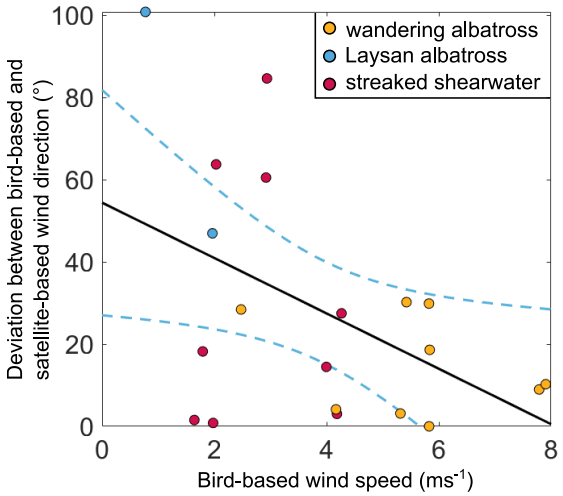

Fig. 2-12. The deviation between bird-based and satellite-based wind direction in relation to wind speed.

Color represents streaked shearwaters (red), Laysan albatrosses (blue), and wandering albatrosses (orange). Deviation between bird-based and satellite-based wind estimated increases as wind speed becomes weaker (Pearson's $R = 0.48$, $P < 0.03$).

Chapter 3

Adjustment of flight pattern in response to wind of seabirds combining flapping and dynamic soaring

本章（項）の内容は、学術雑誌論文として出版する計画があるため公表できない。5 年以内に出版予定。

Chapter 4

General Discussion

本章（項）の内容は、学術雑誌論文として出版する計画があるため公表できない。5 年以内に出版予定。

Acknowledgement

本研究を遂行するにあたり、研究の計画から論文の執筆に至るまで、ご指導ご鞭撻を賜りました東京大学大気海洋研究所の佐藤克文教授に心から感謝いたします。

本研究では、岩手県山田町船越大島でのオオミズナギドリ調査を行うにあたり、多くの方にお世話になりました。とりわけ、山田町田之浜の漁師阿部辰男氏、阿部貴徳氏には島への送迎や物品管理など、調査全体にわたりご協力いただきました。野外調査は同研究室の塩見こずえ氏（現：国立極地研究所助教)、後藤佑介氏、坂尾美帆氏のオオミズナギドリ研究チームの協力で実施することができました。また、船越大島での調査協力をしていただいた名古屋大学の海鳥研究メンバーの依田憲教授、塩崎達也氏、菅原貴徳氏、に深く感謝いたします。岩手での調査で拠点としていた東京大学大気海洋研究所国際沿岸海洋研究センターの皆様には調査期間中温かいお言葉をいただきましたことを感謝いたします。

本研究ではハワイで繁殖するコアホウドリの調査を行うにあたり、多くの方にお世話になりました。ハワイでのコアホウドリ研究に携わる機会を提供してくださり、プロジェクトの総括をして頂いた北海道大学の綿貫豊教授に心より感謝申し上げます。2014 年度の調査でデータを取得して頂いた後藤佑介氏にお礼申し上げます。また、2015 年度の調査で現場の総括をしていただいた西沢文吾氏、現地での調査協力をしていただいた菅原貴徳氏、山下麗氏にお礼申し上げます。

本博士論文の内容に関する原著論文を執筆するにあたり、後藤佑介氏に解析に関する多くの助言をいただいたことを深く感謝いたします。また、依田憲教授、綿貫豊教授、Lindsay C. Young 博士、Henri Weimerskirch 博士、Charles-André Bost 博士には、共著者として原著論文作成に当たり多くのアドバイスをいただきました。心よりお礼申し上げます。また、本博士論文を副査として査読してくださった、河村知彦教授、小松幸生准教授、山川卓准教授、綿貫豊教授にお礼申し上げます。

研究生活において支えとなって頂いた大気海洋研究所行動生態計測分野佐藤研究室の皆様には心からお礼申し上げます。最後に、常に応援していただいた家族に心より感謝いたします。

References

Adams, J. and Flora, S. (2009). Correlating seabird movements with ocean winds: linking satellite telemetry with ocean scatterometry. *Mar. Biol.* **157**, 915–929.

Albert, A., Echevin, V., Lévy, M. and Aumont, O. (2010). Impact of nearshore wind stress curl on coastal circulation and primary productivity in the Peru upwelling system. *J. Geophys. Res.* **115**, C12033.

Alexander, R. M. (2003). *Principles of animal locomotion*. Princeton University Press.

Amélineau, F., Péron, C., Lescroël, A., Authier, M., Provost, P. and Grémillet, D. (2014). Windscape and tortuosity shape the flight costs of northern gannets. *J. Exp. Biol.* **217**, 876–85.

Bevan, R. M., Butler, P. J., Woakes, A. J. and Prince, P. A. (1995). The energy expenditure of free-ranging black-browed albatrosses. *Philos. Trans. Biol. Sci.* **350**, 119–131.

Biuw, M., Boehme, L., Guinet, C., Hindell, M., Costa, D., Charrassin, J.-B., Roquet, F., Bailleul, F., Meredith, M., Thorpe, S., et al. (2007). Variations in behavior and condition of a Southern Ocean top predator in relation to in situ oceanographic conditions. *Proc. Natl. Acad. Sci. USA* **104**, 13705–13710.

Bousquet, G. D., Triantafyllou, M. S. and Slotine, J.-J. E. (2017). Optimal dynamic soaring consists of successive shallow arcs. *J. R. Soc. Interface* **14**, 20170496.

Bower, G. (2011). Boundary layer dynamic soaring for autonomous aircraft: design and validation. In *PhD thesis*, p. Stanford University, Stanford, USA.

Catry, P., Phillips, R. A. and Croxall, J. P. (2004). Sustained fast travel by a gray-headed albatross (*Thalassarche chrysostoma*) riding an Antarctic storm. *Auk* **121**, 1208–1213.

Charrassin, J.-B., Park, Y.-H., Le Maho, Y. and Bost, C.-A. (2002). Penguins as oceanographers unravel hidden mechanisms of marine productivity. *Ecol. Lett.* **5**, 317–319.

Charrassin, J.-B., Hindell, M., Rintoul, S. R., Roquet, F., Sokolov, S., Biuw, M., Costa, D., Boehme, L., Lovell, P., Coleman, R., et al. (2008). Southern Ocean frontal structure and sea-ice formation rates revealed by elephant seals. *Proc. Natl. Acad. Sci. USA* **105**, 11634–11639.

Chelton, D. B., Schlax, M. G., Freilich, M. H. and Milliff, R. F. (2004). Satellite measurements reveal persistent small-scale features in ocean winds. *Science* **303**, 978–983.

Chelton, D. B., Freilich, M. H., Sienkiewicz, J. M. and Von Ahn, J. M. (2006). On the use of QuikSCAT scatterometer measurements of surface winds for marine weather prediction. *Mon. Weather Rev.* **134**, 2055–2071.

Crosby, D. S., Breaker, L. C. and Gemmill, W. H. (1993). A proposed definition for vector correlation in geophysics - theory and application. *J. Atmos. Ocean. Technol.* **10**, 355–367.

Durant, J., Hjermann, D., Frederiksen, M., Charrassin, J., Le Maho, Y., Sabarros, P., Crawford, R. and Stenseth, N. (2009). Pros and cons of using seabirds as ecological indicators. *Clim. Res.* **39**, 115–129.

Ebuchi, N., Graber, H. C. and Caruso, M. J. (2002). Evaluation of wind vectors observed by

QuikSCAT/SeaWinds using ocean buoy data. *J. Atmos. Ocean. Technol.* **19**, 2049–2062.

Egevang, C., Stenhouse, I. J., Phillips, R. A., Petersen, A., Fox, J. W. and Silk, J. R. D. (2010). Tracking of Arctic terns *Sterna paradisaea* reveals longest animal migration. *Proc. Natl. Acad. Sci. U. S. A.* **107**, 2078–81.

Elliott, K. H. and Gaston, A. J. (2005). Flight speeds of two seabirds: A test of Norberg's hypothesis. *Ibis (Lond. 1859).* **147**, 783–789.

Elliott, K. H., Chivers, L. S., Bessey, L., Gaston, A. J., Hatch, S. A., Kato, A., Osborne, O., Ropert-Coudert, Y., Speakman, J. R. and Hare, J. F. (2014). Windscapes shape seabird instantaneous energy costs but adult behavior buffers impact on offspring. *Mov. Ecol.* **2**, 17.

Freilich, M. H. and Dunbar, R. S. (1999). The accuracy of the NSCAT 1 vector winds: Comparisons with National Data Buoy Center buoys. *J. Geophys. Res.* **104**, 11231.

Gibb, R., Shoji, A., Fayet, A. L., Perrins, C. M., Guilford, T. and Freeman, R. (2017). Remotely sensed wind speed predicts soaring behaviour in a wide-ranging pelagic seabird. *J. R. Soc. Interface* **14**, 20170262.

Goto, Y., Yoda, K. and Sato, K. (2017). Asymmetry hidden in birds' tracks reveals wind, heading, and orientation ability over the ocean. *Sci. Adv.* **3**, e1700097.

Hays, G. C., Ferreira, L. C., Sequeira, A. M. M., Meekan, M. G., Duarte, C. M., Bailey, H., Bailleul, F., Bowen, W. D., Caley, M. J., Costa, D. P., et al. (2016). Key questions in marine megafauna movement ecology. *Trends Ecol. Evol.* **31**, 463–475.

He, R., Liu, Y. and Weisberg, R. H. (2004). Coastal ocean wind fields gauged against the performance of an ocean circulation model. *Geophys. Res. Lett.* **31**, L14303.

Hedenstrom, A. and Alerstam, T. (1995). Optimal Flight Speed of Birds. *Philos. Trans. R. Soc. B Biol. Sci.* **348**, 471–487.

Hedenström, A. and Åkesson, S. (2017). Adaptive airspeed adjustment and compensation for wind drift in the common swift: differences between day and night. *Anim. Behav.* **127**, 117–123.

Hedenström, A., Alerstam, T., Green, M. and Gudmundsson, G. A. (2002). Adaptive variation of airspeed in relation to wind, altitude and climb rate by migrating birds in the Arctic. *Behav. Ecol. Sociobiol.* **52**, 308–317.

Horvitz, N., Sapir, N., Liechti, F., Avissar, R., Mahrer, I. and Nathan, R. (2014). The gliding speed of migrating birds: slow and safe or fast and risky? *Ecol. Lett.* **17**, 670–679.

Kawai, Y., Miyama, T., Iizuka, S., Manda, A., Yoshioka, M. K., Katagiri, S., Tachibana, Y. and Nakamura, H. (2015). Marine atmospheric boundary layer and low-level cloud responses to the Kuroshio Extension front in the early summer of 2012: three-vessel simultaneous observations and numerical simulations. *J. Oceanogr.* **71**, 511–526.

Kogure, Y., Sato, K., Watanuki, Y., Wanless, S. and Daunt, F. (2016). European shags optimize their flight behavior according to wind conditions. *J. Exp. Biol.* **219**, 311–318.

Lawrance, N. R. J. and Sukkarieh, S. (2010). Simultaneous exploration and exploitation of a wind field for a small gliding UAV. *Proc. AIAA Guid. Navig. Control Conf.*

Liechti, F. (2006). Birds: blowin' by the wind? *J. Ornithol.* **147**, 202–211.

Liechti, F., Hedenström, A. and Alerstam, T. (1994). Effects of sidewinds on optimal flights speed of birds. *J. Theor. Biol.* **170**, 219–225.

Liu, W. T. (2002). Progress in scatterometer application. *J. Oceanogr.* **58**, 121–136.

McLaren, J. D., Shamoun-Baranes, J., Camphuysen, C. J. and Bouten, W. (2016). Directed flight and optimal airspeeds: homeward-bound gulls react flexibly to wind yet fly slower than predicted. *J. Avian Biol.* **47**, 476–490.

Miyazawa, Y., Guo, X., Varlamov, S. M., Miyama, T., Yoda, K., Sato, K., Kano, T. and Sato, K. (2015). Assimilation of the seabird and ship drift data in the north-eastern sea of Japan into an operational ocean nowcast/forecast system. *Sci. Rep.* **5**, 17672.

Norberg, U. M. (Ulla M. . (1990). *Vertebrate Flight : Mechanics, Physiology, Morphology, Ecology and Evolution*. Springer Berlin Heidelberg.

Passing, H. and Bablok, W. (1983). A new biometrical procedure for testing the equality of measurements from 2 different analytical methods - application of linear-regression procedures for method comparison studies in clinical chemistry .1. *J. Clin. Chem. Clin. Biochem.* **21**, 709–720.

Penhallurick, J. and Wink, M. (2004). Analysis of the taxonomy and nomenclature of the Procellariiformes based on complete nucleotide sequences of the mitochondrial cytochrome *b* gene. *Emu - Austral Ornithol.* **104**, 125–147.

Pennycuick, C. J. (1978). Fifteen testable predictions about bird flight. *Oikos* **30**, 165–176.

Pennycuick, C. J. (1982). The flight of petrels and albatrosses (Procellariiformes), observed in South Georgia and its vicinity. *Philos. Trans. R. Soc. B Biol. Sci.* **300**, 75–106.

Pennycuick, C. J. (1987). Flight of auks (Alcidae) and other northern seabirds compared with southern Procellariiformes: ornithodolite observations. *J. Exp. Biol.* **128**, 335–347.

Pennycuick, C. J. (2002). Gust soaring as a basis for the flight of petrels and albatrosses (Procellariiformes). *Avian Sci.* **2**, 1–12.

Pennycuick, C. J. (2008). *Modelling the flying bird*. Amsterdam, The Netherlands: Academic Press.

Pickett, M. H., Tang, W., Rosenfeld, L. K. and Wash, C. H. (2003). QuikSCAT satellite comparisons with nearshore buoy wind data off the U.S. west coast. *J. Atmos. Ocean. Technol.* **20**, 1869–1879.

Rayleigh, J. W. S. (1883). The soaring of birds. *Nature* **27**, 534–535.

Rayner, J. M. V. (1991). On the aerodynamics of animal flight in ground effect. *Philos. Trans. R. Soc. B Biol. Sci.* **334**, 119–128.

Richardson, P. L. (2011). How do albatrosses fly around the world without flapping their wings? *Prog. Oceanogr.* **88**, 46–58.

Richardson, P. L. (2015). Upwind dynamic soaring of albatrosses and UAVs. *Prog. Oceanogr.* **130**, 146–156.

Roquet, F., Wunsch, C., Forget, G., Heimbach, P., Guinet, C., Reverdin, G., Charrassin, J.-B.,

Bailleul, F., Costa, D. P., Huckstadt, L. A., et al. (2013). Estimates of the Southern Ocean general circulation improved by animal-borne instruments. *Geophys. Res. Lett.* **40**, 6176–6180.

Rosén, M. and Hedenström, A. (2001). Testing predictions from flight mechanical theory: A case study of Cory's shearwater and Audouin's gull. *Acta Ethol.* **3**, 135–140.

Rykaczewski, R. R. and Checkley, D. M. (2008). Influence of ocean winds on the pelagic ecosystem in upwelling regions. *Proc. Natl. Acad. Sci. USA* **105**, 1965–1970.

Sachs, G. (2005). Minimum shear wind strength required for dynamic soaring of albatrosses. *Ibis (Lond. 1859).* **147**, 1–10.

Sachs, G., Traugott, J. and Holzapfel, F. (2011). Progress against the wind with dynamic soaring–results from in-flight measurements of albatrosses–. *Am. Inst. Aeronaut. Astronaut. AIAA 2011-6225*.

Sachs, G., Traugott, J., Nesterova, A. P., Dell'Omo, G., Kümmeth, F., Heidrich, W., Vyssotski, A. L. and Bonadonna, F. (2012). Flying at no mechanical energy cost: disclosing the secret of wandering albatrosses. *PLoS One* **7**, e41449.

Sachs, G., Traugott, J., Nesterova, A. P. and Bonadonna, F. (2013). Experimental verification of dynamic soaring in albatrosses. *J. Exp. Biol.* **216**, 4222–4232.

Sakamoto, K. Q., Takahashi, A., Iwata, T., Yamamoto, T., Yamamoto, M. and Trathan, P. N. (2013). Heart rate and estimated energy expenditure of flapping and gliding in black-browed albatrosses. *J. Exp. Biol.* **216**, 3175–3182.

Sapir, N., Horvitz, N., Dechmann, D. K. N., Fahr, J. and Wikelski, M. (2014). Commuting fruit bats beneficially modulate their flight in relation to wind. *Proc. R. Soc. B Biol. Sci.* **281**, 20140018–20140018.

Sato, K., Sakamoto, K. Q., Watanuki, Y., Takahashi, A., Katsumata, N., Bost, C. A. and Weimerskirch, H. (2009). Scaling of soaring seabirds and implications for flight abilities of giant pterosaurs. *PLoS One* **4**, e5400.

Shaffer, S. A., Tremblay, Y., Weimerskirch, H., Scott, D., Thompson, D. R., Sagar, P. M., Moller, H., Taylor, G. A., Foley, D. G., Block, B. A., et al. (2006). Migratory shearwaters integrate oceanic resources across the Pacific Ocean in an endless summer. *Proc. Natl. Acad. Sci.* **103**, 12799–12802.

Shamoun-Baranes, J., van Loon, E., Liechti, F. and Bouten, W. (2007). Analyzing the effect of wind on flight: pitfalls and solutions. *J. Exp. Biol.* **210**, 82–90.

Shimatani, I. K., Yoda, K., Katsumata, N. and Sato, K. (2012). Toward the quantification of a conceptual framework for movement ecology using circular statistical modeling. *PLoS One* **7**, e50309.

Shiomi, K., Yoda, K., Katsumata, N. and Sato, K. (2012). Temporal tuning of homeward flights in seabirds. *Anim. Behav.* **83**, 355–359.

Shirai, M., Yamamoto, M., Ebine, N., Yamamoto, T., Trathan, P. N., Yoda, K., Oka, N. and Niizuma, Y. (2012). Basal and field metabolic rates of streaked shearwater during the

chick-rearing period. *Ornithol. Sci.* **11**, 47–55.

Spear, L. B. and Ainley, D. G. (1997). Flight speed of seabirds in relation to wind speed and direction. *Ibis (Lond. 1859).* **139**, 234–251.

Spivey, R. J., Stansfield, S. and Bishop, C. M. (2014). Analysing the intermittent flapping flight of a Manx shearwater, Puffinus puffinus, and its sporadic use of a wave-meandering wing-sailing flight strategy. *Prog. Oceanogr.* **125**, 62–73.

Streby, H. M., Kramer, G. R., Peterson, S. M., Lehman, J. A., Buehler, D. A. and Andersen, D. E. (2015). Tornadic storm avoidance behavior in breeding songbirds. *Curr. Biol.* **25**, 98–102.

Stull, R. B. (2003). *An Introduction to Boundary Layer Meteorology*. Dordrecht, The Netherlands: Kluwer Academic Publishers.

Suryan, R. M., Anderson, D. J., Shaffer, S. A., Roby, D. D., Tremblay, Y., Costa, D. P., Sievert, P. R., Sato, F., Ozaki, K., Balogh, G. R., et al. (2008). Wind, waves, and wing loading: Morphological specialization may limit range expansion of endangered albatrosses. *PLoS One* **3**,.

Taylor, G. K., Reynolds, K. V and Thomas, A. L. R. (2016). Soaring energetics and glide performance in a moving atmosphere. *Philos. Trans. R. Soc. B Biol. Sci.* **371**, 20150398.

Treep, J., Bohrer, G., Shamoun-Baranes, J., Duriez, O., Prata de Moraes Frasson, R. and Bouten, W. (2015). Using high resolution GPS tracking data of bird flight for meteorological observations. *Bull. Am. Meteorol. Soc.* BAMS-D-14-00234.1.

Vansteelant, W. M. G., Shamoun-Baranes, J., McLaren, J., van Diermen, J. and Bouten, W. (2017). Soaring across continents: decision-making of a soaring migrant under changing atmospheric conditions along an entire flyway. *J. Avian Biol.* **48**, 887–896.

Wada, A., Kunii, M., Yonehara, Y. and Sato, K. (2017). Impacts on local heavy rainfalls of surface winds measurement by seabirds. *CAS/JSC WGNE Res. Act. Atm. Ocean. Model.* **47**, 25.

Watanabe, Y. Y., Takahashi, A., Sato, K., Viviant, M. and Bost, C.-A. (2011). Poor flight performance in deep-diving cormorants. *J. Exp. Biol.* **214**, 412–21.

Weimerskirch, H., Wilson, R., Guinet, C. and Koudil, M. (1995). Use of seabirds to monitor sea-surface temperatures and to validate satellite remote-sensing measurements in the Southern Ocean. *Mar. Ecol. Prog. Ser.* **126**, 299–303.

Weimerskirch, H., Guionnet, T., Martin, J., Shaffer, S. A. and Costa, D. P. (2000). Fast and fuel efficient? Optimal use of wind by flying albatrosses. *Proc. R. Soc. B* **267**, 1869–1874.

Weimerskirch, H., Bonadonna, F., Bailleul, F., Mabille, G., Dell'Omo, G. and Lipp, H.-P. (2002). GPS tracking of foraging albatrosses. *Science* **295**, 1259.

Weimerskirch, H., Louzao, M., de Grissac, S. and Delord, K. (2012). Changes in wind pattern alter albatross distribution and life-history traits. *Science* **335**, 211–214.

Weimerskirch, H., Cherel, Y., Delord, K., Jaeger, A., Patrick, S. C. and Riotte-Lambert, L. (2014). Lifetime foraging patterns of the wandering albatross: Life on the move! *J. Exp. Mar. Bio. Ecol.* **450**, 68–78.

Weimerskirch, H., Delord, K., Guitteaud, A., Phillips, R. A. and Pinet, P. (2015). Extreme

variation in migration strategies between and within wandering albatross populations during their sabbatical year, and their fitness consequences. *Sci. Rep.* **5**, 8853.

Weimerskirch, H., Bishop, C., Jeanniard-du-Dot, T., Prudor, A. and Sachs, G. (2016). Frigate birds track atmospheric conditions over months-long transoceanic flights. *Science.* **353**, 74–78.

Weinzierl, R., Bohrer, G., Kranstauber, B., Fiedler, W., Wikelski, M. and Flack, A. (2016). Wind estimation based on thermal soaring of birds. *Ecol. Evol.* **6**, 8706–8718.

Wilmers, C. C., Nickel, B., Bryce, C. M., Smith, J. A., Wheat, R. E., Yovovich, V. and Hebblewhite, M. (2015). The golden age of bio-logging: How animal-borne sensors are advancing the frontiers of ecology. *Ecology* **96**, 1741–1753.

Wilson, R., Grémillet, D., Syder, J., Kierspel, M., Garthe, S., Weimerskirch, H., Schäfer-Neth, C., Scolaro, J., Bost, C., Plötz, J., et al. (2002). Remote-sensing systems and seabirds: their use, abuse and potential for measuring marine environmental variables. *Mar. Ecol. Prog. Ser.* **228**, 241–261.

Yamamoto, T., Takahashi, A., Oka, N., Iida, T., Katsumata, N., Sato, K. and Trathan, P. N. (2011). Foraging areas of streaked shearwaters in relation to seasonal changes in the marine environment of the Northwestern Pacific: Inter-colony and sex-related differences. *Mar. Ecol. Prog. Ser.* **424**, 191–204.

Yoda, K., Shiomi, K. and Sato, K. (2014). Foraging spots of streaked shearwaters in relation to ocean surface currents as identified using their drift movements. *Prog. Oceanogr.* **122**, 54–64.

Yonehara, Y., Goto, Y., Yoda, K., Watanuki, Y., Young, L. C., Weimerskirch, H., Bost, C.-A. and Sato, K. (2016). Flight paths of seabirds soaring over the ocean surface enable measurement of fine-scale wind speed and direction. *Proc. Natl. Acad. Sci. U. S. A.* **113**, 9039–44.

Young, I. R., Zieger, S. and Babanin, A. V. (2011). Global trends in wind speed and wave height. *Science* **332**, 451–455.

Zar, H. J. (1999). *Biostatistical analysis*. fourth edi. Prentice Hall.

Zhao, Y. J. (2004). Optimal patterns of glider dynamic soaring. *Optim. Control Appl. Methods* **25**, 67–89.

Zhao, Y. J. and Qi, Y. C. (2004). Minimum fuel powered dynamic soaring of unmanned aerial vehicles utilizing wind gradients. *Optim. Control Appl. Methods* **25**, 211–233.